

Toward Energy-Efficient Multiple IRSs: Federated Learning-Based Configuration Optimization

Lixin Li¹, Member, IEEE, Donghui Ma, Huan Ren, Peijue Wang, Wensheng Lin², Member, IEEE, and Zhu Han³, Fellow, IEEE

Abstract—Intelligent reflecting surface (IRS) can enhance the capacity and cost-effectiveness in future wireless networks substantially. However, the configuration optimization of IRS in an energy-efficient way is still a challenging work. In this paper, we propose a solution to the problem of maximizing the total throughput of a multiple IRSs assisted multi-user communication system. A federated deep learning (FDL) based algorithm is designed to obtain the optimal reflection configurations of all IRSs in parallel, where the model parameters are transmitted instead of the dataset itself as in deep learning (DL). Specifically, a deep neural network (DNN) is formulated to fit the coupling relationship between the coordinate information of users and the optimal reflecting vector of IRS. Meanwhile, the analysis of transmission and computation overhead is performed to establish an accurate energy consumption model. For performance evaluation, we conduct a series of simulations to verify the effectiveness of the FDL framework. The simulation results demonstrate that the test accuracy of the FDL framework is as high as 95.22% with only 1/36 of the transmission energy consumption compared with the DL. Moreover, the total throughput can achieve 93% of the theoretical performance.

Index Terms—Intelligent reflecting surfaces, energy efficiency, federated learning, deep learning.

I. INTRODUCTION

THE FUTURE wireless communication networks focus on two issues, i.e., user experience and cost-effectiveness. As a revolutionary technique, intelligent reflecting surfaces (IRSs) improve the transmission capacity and the rate of existing wireless networks as a reflective device without

changing the standardization and hardware of existing wireless communications [1]–[3]. Specifically, IRS can reshape the propagation environment by adjusting electromagnetic responses (e.g., amplitude, phase, frequency, etc.). The combination of IRSs and wireless communication technologies, e.g., beamforming [4]–[7], millimeter-wave (mmWave) communication [8], [9], channel estimation [10], [11], source allocation [12], [13] and secure wireless communication [14], [15], provides a promising solution with high user experience and cost-effectiveness in the future wireless communications. Due to the obstacles of non-line-of-sight (NLoS) links and the uncontrollability of wireless channel in the communication scenarios, the IRSs are integrated into existing networks because of its passive array, reflective mechanisms, flexible deployment, and cost-effectiveness.

For the IRS enabled scenarios, such as secure communication, throughput improvement, and the virtual line-of-sight (LoS) link construction, the optimization of reflection coefficient is indispensable. Remarkably, there are already some positive results based on convex optimization, both in the design of IRS reflection coefficient and the joint optimization with beamforming. However, a single IRS is not enough to support the needs of task-intensive scenarios (e.g., stadium, concert), when an IRS group needs to be considered. At this point, the optimization task is transformed into computationally intensive, in other words, the computational overhead of convex optimization-based methods becomes unaffordable, which poses a great challenge to the real-time performance and robustness of IRS-assisted communication systems.

In this context, deep learning (DL) is introduced into IRS-assisted wireless communication system design due to its compelling end-to-end mapping properties. Nevertheless, the training process of DL requires that all training data be gathered and stored on a specific device, which is called a central server. Concurrently, the generally large volume of training data means that when the communication environment is not ideal, it may cause an unexpected transmission burden or even congestion or interruption, which can greatly affect the training effect of the network. In addition, this centralized collection pattern will cause the risk of privacy leakage in some cases.

Therefore, how to find a satisfactory compromise between computing-intensive and transmission-intensive is a challenging problem. Federated learning (FL) is a solution, i.e., instead of sending raw data to the central server, each participant trains the local model by utilizing their own data and sends the updated model parameters for aggregation. This is the reason

Manuscript received May 31, 2021; revised October 17, 2021 and December 1, 2021; accepted December 12, 2021. Date of publication December 17, 2021; date of current version May 20, 2022. This work was supported in part by the Key Research and Development Plan of Shaanxi Province under Grant 2020GY-034; in part by the National Natural Science Foundation of China (NSFC) under Grant 62001387; in part by the Shanghai Academy of Spaceflight Technology (SAST) under Grant SAST2020124; in part by the Fundamental Research Funds for the Central Universities; in part by NSF under Grant CNS-2128368 and Grant CNS-2107216; in part by Toyota; and in part by Amazon. (Corresponding authors: Lixin Li; Wensheng Lin.)

Lixin Li, Donghui Ma, Peijue Wang, and Wensheng Lin are with the School of Electronics and Information, Northwestern Polytechnical University, Xi'an 710129, Shaanxi, China (e-mail: lilixin@nwpu.edu.cn; ma2507441744@mail.nwpu.edu.cn; pjw666@mail.nwpu.edu.cn; linwest@nwpu.edu.cn).

Huan Ren is with the Beijing Institute of Telemetry Technology, Beijing 100094, China (e-mail: rh2541@mail.nwpu.edu.cn).

Zhu Han is with the Department of Electrical and Computer Engineering, University of Houston, Houston, TX 77004 USA, and also with the Department of Computer Science and Engineering, Kyung Hee University, Seoul 446-701, South Korea (e-mail: zhan2@uh.edu).

Digital Object Identifier 10.1109/TGCN.2021.3136306

that FL can significantly reduce the transmission burden and the risk of privacy leakage. At the same time, FL keeps the aforementioned advantages of DL.

In this paper, we aim at indoor mmWave downlink communications where a wireless access point (AP) is assisted by multiple IRSs to ensure frequent services for high-density single-antenna users. Based on the indoor scenario, an energy efficient federated DL (FDL) framework is established to implement the parallel configuration of multiple IRSs. The FDL framework trains multiple neural networks in parallel, which guarantees seamless and instant connection of high-mobility users with corresponding IRS. Besides, the proposed algorithm performs lower computational complexity and higher energy efficiency compared with some classic methods. Specifically, the encrypted local models are uploaded to the federated central server, and then the global model is trained in the federated central server by integrating the uploaded local models virtually. To establish an accurate energy consumption model, the analysis of transmission and computation overhead under different schemes is also performed.

The contributions in this paper are summarized as follows.

- 1) This paper establishes an energy-efficient FDL framework for the configuration optimization of multiple IRSs in high-density networks. In the FDL framework, each IRS transmits the neural network model after local training rather than the raw local dataset. By this means, the system can significantly reduce the communication burden and the energy consumption, while keeping the total throughput close to the performance limit obtained by exhaustive search.
- 2) To find the optimal configuration efficiently, we design a deep neural network (DNN) model to establish the mapping relationship from the users' coordinate information to the optimal configuration of an IRS. Compared to exhaustive search, the designed DNN is able to obtain sufficiently accurate IRS configurations for maximizing system performance, without huge computation cost.
- 3) Moreover, we construct a general energy consumption model for evaluating the energy efficiency of DL and FDL. The energy consumption is analyzed in detail in terms of transmission and computation.
- 4) Finally, a series of simulations are conducted to verify the effectiveness of the proposed FDL framework. The simulation results indicate that with an extremely low energy consumption, the FDL algorithm can still achieve approximately 93% of the theoretical throughput limit. Consequently, the FDL framework is verified to be highly energy-efficient for the configuration optimization of multiple IRSs in high-density networks.

The rest of the paper is organized as follows. In Section II, the related works are discussed in the literature. Section III introduces the system model of the indoor communication network with an AP assisted by multiple IRSs. Section IV presents the energy consumption model, composition and generation of the training dataset, and the specific process of FDL in detail. To evaluate the performance of the FDL network,

TABLE I
THE LIST OF MAIN NOTATIONS

Notation	Definition
S	Number of IRSs
K	Total number of users
M	Transmitting antennas of AP
N	Total number of IRS reflecting elements
N_y	The number of IRS elements that distributed on the y -axis
N_z	The number of IRS elements that distributed on the z -axis
\mathbf{h}_t^s	The channel from AP to s -th IRS
$\mathbf{h}_r^{s,k}$	The channel from user k to s -th IRS
\mathbf{H}^k	The channel from AP to user k
Θ	Reflection coefficient diagonal matrix at the IRS
$\tilde{\Theta}_{out}$	The real output of neural network
Θ_{opt}	The optimal reflection coefficient matrix of IRS
$\alpha_{r,l}$	Beam steering vectors of IRS over l -th path
$\alpha_{t,l}$	Beam steering vectors of AP over l -th path
\mathbf{O}_s	Local dataset of smart controller s
\mathbf{W}_s^i	local model of smart controller s in the i -th round
\mathbf{W}^i	The global model for i -th training round
\mathbf{W}_{opt}	The optimal model
Ψ_s	The local dataset of s -th IRS
Ω	The input of neural network
ρ	Learning rate
E^t	The transmission energy consumption
E^c	The computation energy consumption

Section V conducts a series simulations. Finally, the conclusion is drawn in Section VI. Moreover, we list the adopted notations throughout this paper in Table I for clarity.

II. RELATED WORK

Energy efficiency is a critical performance indicator in IRS-assisted wireless communications [16]–[18]. And there has been some priors work about the energy efficiency maximization of the IRS-assisted communication system. In the past decade, some classic optimization methods and learning techniques are sufficiently attractive for configuring the IRS to explore the field of maximizing energy efficiency. In this section, we will review and discuss them in detail and these studies are concluded in Table II.

Jia *et al.* [19] placed an IRS to aid device-to-device (D2D) communication network. An energy efficiency maximization problem was investigated in the above scenario, which was decoupled into two subproblems and optimized alternately. It was demonstrated that the algorithm could significantly improve the energy efficiency of the D2D network. Sun *et al.* [20] deployed multiple IRSs to assisted multi-user multiple-input single-output (MISO) downlink cellular network. They took the circuit power of the IRS into consideration on the condition that the number of the reflecting elements is large. The phase of the IRSs and the beamforming vectors of the base station (BS) were jointly optimized to maximize energy efficiency. Zhou *et al.* [21] showed that

TABLE II
SUMMARY OF EXISTING WORKS

Ref.	Algorithm	Description
[23]	SCA	Joint optimization of the on-off status and the reflection coefficients.
[24]	MMSE, MM	Non-trivial tradeoff between the energy efficiency and the spectral efficiency.
[19]	SDR, Dinkelbach	Decouple and alternating optimization.
[20]	SDR, BR	Minimize the network power consumption (involving the circuit power of IRS).
[25], [27]	RL	Maximize the average energy efficiency / capacity.
[26], [28]	DL	Reducing the transmission overhead. Maximizing throughput.
[29]	FL	Maximizing the achievable rate.

the maximization of energy efficiency may lead to a loss of spectral efficiency. They analyzed the spectral and energy efficiency of an IRS-assisted MISO downlink system with hardware impairments at both the BS and IRS. For maximizing the energy efficiency, the optimal solution of transmit power was obtained and increased with the radio-frequency (RF) impairments. Xiong *et al.* [22] aimed at multiuser multiple-input multiple-output (MIMO) uplink transmission aided by an IRS equipped with discrete phase shifters, in which the tradeoff between energy efficiency and spectral efficiency was considered. Yang *et al.* [23] pointed out a method to maximize the energy efficiency by jointly optimizing the on-off status of each IRS and the corresponding reflection coefficients matrix, the successive convex approximation (SCA) method and the greedy searching are utilized to solve the optimization problem for single user case and multi-user case, separately. To maximize the energy efficiency, they presented a framework that jointly optimized users' transmit precoding and IRS reflective beamforming. You *et al.* [24] investigated the non-trivial tradeoff between the energy efficiency and the spectral efficiency in IRS-assisted MIMO communications. Nonetheless, with the increase of the number of IRS elements, the complexity of these proposed algorithms will be unaffordable. Consequently, new approaches are required to improve the energy efficiency in IRS-assisted wireless communications while ensuring practicality and robustness.

On the other hand, DL or reinforcement learning (RL) is considered as the tool to solve the optimization problem of reflecting coefficients configuration for IRS independently or jointly [25]–[29]. Lee *et al.* [25] considered an IRS-assisted cellular network endowed with an IRS reflector powered via energy harvesting technologies. The author proposed a deep reinforcement learning (DRL) approach to maximize the average energy efficiency, which demonstrated outstanding energy efficiency performance with the increase of IRS elements. Khan and Shin [26] proposed a DL approach to estimate channels and phase angles of the reflected signal via an IRS, in which the network utilizes fully connected layers. This method achieved improvements in terms of the bit error rate and was proved to be able to reduce the transmission

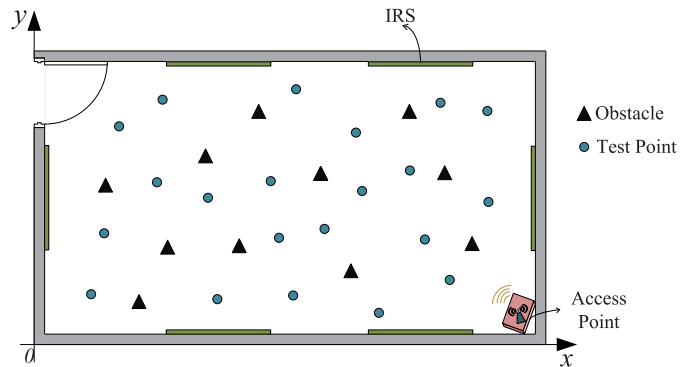


Fig. 1. Multiple IRSs-assisted AP for the indoor communication network.

overhead. Zhang *et al.* [27] presented a joint optimization problem with respect to the location and reflection coefficients of an unmanned aerial vehicle (UAV) in a UAV-assisted ground BS mmWave network, where the Q-learning and neural network-based RL method was adopted to model the propagation environment for maximizing downlink transmission capacity. To this effect, it was demonstrated that the use of RL-based deployment of the UAV-IRS achieved outstanding performance. Huang *et al.* [28] designed an effective online wireless configuration problem in the single IRS-assisted AP indoor communication environment, in which the authors utilized DL to output the optimal phase configurations for maximizing system throughput. Ma *et al.* [29] developed the distributed rate optimization with FL in an IRS-assisted BS, which demonstrated significant performance improvement in terms of achievable system rate. Nonetheless, those above prior works have been studied on single IRS-assisted point-to-point communications by ground BS, and the achievements in the previous literature cannot be simply extended to the wireless networks assisted by multiple IRSs.

III. SYSTEM MODEL AND PROBLEM FORMULATION

As illustrated in Fig. 1, we consider a two-dimensional (2D) top view of the three-dimensional (3D) indoor environment with multiple IRSs that are installed on the wall. The test

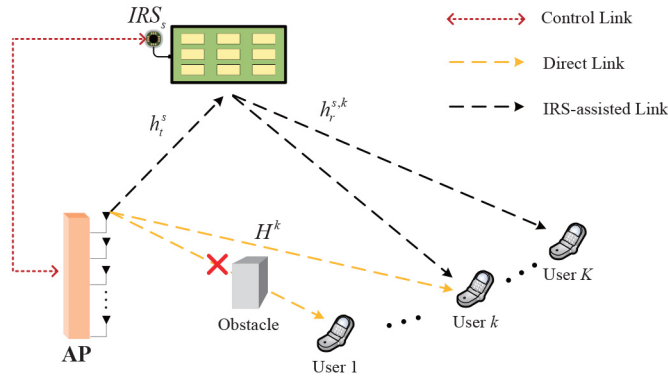


Fig. 2. Single IRS-assisted AP for the indoor mmWave communication model.

points represent the possible location coordinates of mobile users. Due to the complex indoor environment, there are some obstacles blocking direct links between the AP and the users. Consequently, the deployment of multiple IRSs creates virtual line-of-sight (LoS) links between the AP and the users to maintain connection by bypassing obstacles.

A. Signal Model

In Fig. 1, there are S IRSs identified by the index $S = \{1, 2, \dots, S\}$ and each of them is assumed to be capable of covering the entire area, which means that each user will be assisted by all IRSs. In the indoor communication network, the total number of users is K .

As shown in Fig. 2, a single IRS-assisted AP serving a group of indoor users is regarded as an object for detailed analysis from Fig. 1. Note that the analysis of single IRS-assisted communication can be extended to the case multiple IRSs. Specifically, an AP with M transmitting antennas serves K single-antenna ground users, and the IRS s with N reflecting elements is deployed. Besides, each IRS is connected with a smart controller, responsible for data storage, model training, and IRS reconfiguration. In practice, the computing server can meet the above requirements. The channel from AP and user k to s -th IRS are denoted as $\mathbf{h}_t^s \in \mathbb{C}^{N \times M}$ and $\mathbf{h}_r^{s,k} \in \mathbb{C}^{N \times 1}$, respectively. $\mathbf{H}^k \in \mathbb{C}^{1 \times M}$ represents the direct channel from AP to user k . Thus, the received signal at user k can be expressed as

$$y_{k,a} = \left(\sum_{s=1}^S (\mathbf{h}_r^{s,k})^H \Theta^s \mathbf{h}_t^s + \mathbf{H}^k \right) \mathbf{x} + n^k, \quad (1)$$

$(h)^H$ stands for the conjugate transpose of h . $n^k \sim \mathcal{N}(0, \sigma^2)$ models the additive white Gaussian noise (AWGN) vector. \mathbf{x} denotes the transmitting signal from the AP, which can be further written as

$$\mathbf{x} = \sum_{k=1}^K \omega_k s_k, \quad (2)$$

$\omega_k \in \mathbb{C}^{M \times 1}$ is the beamforming vector at the AP. s_k stands for the encoded symbol transmitted to user k .

We define $\Theta = \text{diag}(\mu_1 e^{j\theta_1}, \mu_2 e^{j\theta_2}, \dots, \mu_N e^{j\theta_N}) \in \mathbb{C}^{N \times N}$ as the reflection coefficient diagonal matrix at the

IRS, where $\mu_n \in [0, 1]$ and $\theta_n \in [0, 2\pi)$ ($n = 1, 2, \dots, N$) are the corresponding amplitude coefficient and phase shift of the n -th reflecting element, respectively. For the sake of simplicity, the effect of amplitude coefficient is normalized in this paper (i.e., $\mu_1 = \mu_2 = \dots = \mu_N = 1$).

B. Channel Model

In this paper, the Saleh-Valenzuela (SV) channel is adopted [30]. The S-V channel model is a statistical model of multi-path channels that accurately reflects the indoor electromagnetic distribution characteristics, which is adopted in the IEEE standard 802.15.3c and it can describe the space-time characteristics of the MIMO communication or IRS-assisted communications. Furthermore, the AP and IRS are modeled as uniform linear array (ULA) and uniform planar array (UPA), respectively.

Then, the channel $\mathbf{h}_r^{s,k}$ and \mathbf{H}^k can be written as

$$\mathbf{h}_t^s = \sqrt{\frac{NM}{L}} \sum_{l=0}^L \alpha_l \alpha_{r,l}(\phi^s, \varphi^s) \alpha_{t,l}^H(\psi^s), \quad (3)$$

$$\mathbf{H}^k = \sqrt{\frac{M}{L}} \sum_{l=0}^L \alpha_l \alpha_{t,l}^H(\vartheta^k). \quad (4)$$

The path number is L . $\alpha_{r,l}$ and $\alpha_{t,l}$ are beam steering vectors of IRS and AP over l -th path. $\psi^s, \vartheta^s \in [-\frac{\pi}{2}, \frac{\pi}{2}]$ are the angle-of-departure (AoD) at the AP to s -th IRS and user k , respectively. The azimuth and elevation of angle-of-arrival (AoA) at s -th IRS are denoted as ϕ^s and φ^s .

Under a fixed coordinate system, $\alpha_{r,l}(\phi^s, \varphi^s)$ can be further derived as the combination of the array response along y -axis and z -axis:

$$\alpha_{r,l}(\phi^s, \varphi^s) = \alpha_{y,l}(\phi^s, \varphi^s) \otimes \alpha_{z,l}(\varphi^s), \quad (5)$$

where \otimes stands for the Kronecker product, and

$$\alpha_{z,l}(\varphi^s) = \sqrt{\frac{1}{N_z}} \left[1, e^{j \frac{2\pi}{\lambda} d \cos(\varphi^s)}, \dots, e^{j \frac{2\pi}{\lambda} d (M_z - 1) \cos(\varphi^s)} \right]^H, \quad (6)$$

$$\alpha_{y,l}(\phi^s, \varphi^s) = \sqrt{\frac{1}{N_y}} \left[1, e^{j \frac{2\pi}{\lambda} d \sin(\phi^s) \sin(\varphi^s)}, \dots, e^{j \frac{2\pi}{\lambda} d (M_y - 1) \sin(\phi^s) \sin(\varphi^s)} \right]^H, \quad (7)$$

λ is the wave length and d is the antenna spacing of IRS.

C. Problem Formulation

Based on (1)-(7), the signal-to-interference-plus-noise ratio (SINR) at the intended user k can be expressed as

$$\gamma_k = \frac{\left| \left[\sum_{s=1}^S (\mathbf{h}_r^{s,k})^H \Theta^s \mathbf{h}_t^s + \mathbf{H}^k \right] \omega_k \right|^2}{\sum_{j \neq k}^K \left| \left[\sum_{s=1}^S (\mathbf{h}_r^{s,k})^H \Theta^s \mathbf{h}_t^s + \mathbf{H}^k \right] \omega_j \right|^2 + \sigma^2}. \quad (8)$$

Consequently, the total throughput of this communication system is presented by

$$R = \sum_{k=1}^K \log_2(1 + \gamma_k). \quad (9)$$

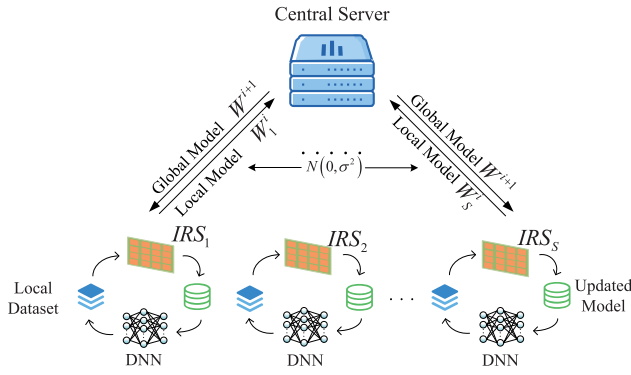


Fig. 3. Federated deep learning framework for multiple IRSs.

In this paper, our goal is to optimize multiple IRSs in an energy-efficient way to further realize the throughput maximization. In other words, these IRSs are optimized in parallel by utilizing FDL. Specifically, a DNN model is jointly established by all IRSs to map the relationship between user distribution and the optimal phase shift configuration of IRS. Therefore, the objective function is given by

$$\begin{aligned} \max \quad & (R, -E) \\ \text{s.t.} \quad & E = E^t + E^c, \\ & \{\Theta_1, \Theta_2, \dots, \Theta_S\}_{opt} = \arg \max_{\Theta_1, \Theta_2, \dots, \Theta_S} \sum_{k=1}^K \log_2(1 + \gamma_k). \end{aligned} \quad (10)$$

The objective function is a binary bundle consisting of two parts: 1) maximization of the total throughput R and 2) minimization of the energy consumption E . The total energy consumption includes the transmission energy consumption E^t and the computation energy consumption E^c , which is analyzed in detail in Section IV.

Besides, the energy consumption model, composition and generation of the training dataset, and the specific process of FDL will be introduced in Section IV.

IV. ENERGY-EFFICIENT CONFIGURATION OPTIMIZATION OF MULTIPLE IRSs

In this section, we establish an FDL framework to realize the optimal configuration of multiple IRSs in the indoor mmWave downlink communication system. Therefore, the DNN for IRS and FDL algorithm for multi-IRS based on the FDL framework is proposed to perform the configuration of IRSs in parallel. Then, the training dataset is introduced detailedly with the aspect of composition and generation. Meanwhile, the analysis of transmission and computation overhead under different schemes is also performed to establish an accurate energy consumption model.

A. FDL Framework

The overall FDL framework is depicted in Fig. 3, where the IRSs fetch each local model update from the federated central server in parallel. The detailed model updating process is described as follows. To begin with, each IRS trains its

local model by using the local dataset. Subsequently, all IRSs upload local updated models to the federated central server in order to perform the model aggregation. Finally, the IRSs download and update the model from the federated central server, and then start the next round of training. Specifically, we adopt the FedAvg algorithm [31] in this paper. The FDL framework consists of three main parts: 1) local model training; 2) encryption mechanism; and 3) model aggregation, of which the details are introduced as follows.

- 1) Local model training: Each local device s (i.e., smart controller, $s = 1, 2, \dots, S$) trains a local DNN model \mathbf{W}_s^i by utilizing its local dataset \mathcal{O}_s in the i -th training round.
- 2) Encryption mechanism: The Gaussian mechanism [32] is adopted to protect the local dataset by adding the Gaussian noise to the gradient of the local models during the training process.
- 3) Model aggregation: As shown in Fig. 3, all local model parameters $\mathbf{W}_1^i, \mathbf{W}_2^i, \dots, \mathbf{W}_S^i$ are transmitted to the central server via an extra link. Then, the global model \mathbf{W}^{i+1} for $(i+1)$ -th training round is generated by aggregating all local models.

Concretely, the local training process can be given by

$$\mathbf{W}_s^i = \mathbf{W}^i - \rho \nabla D_s(\mathbf{W}^i), \quad (11)$$

$$D_s(\mathbf{W}^i) = \frac{1}{|\mathcal{O}_s|} \sum_{j \in \mathcal{O}_s} d_j(\omega), \quad (12)$$

$$d_j(\omega) = \ell(\mathbf{x}_j, \mathbf{y}_j, \omega). \quad (13)$$

In (11), ρ is the learning rate and $\nabla D_s(\mathbf{W}^i)$ is the average gradient on the local data of device s at the current model \mathbf{W}^i . The data scale of device s is indicated by $|\mathcal{O}_s|$ and d_j represents the loss of the prediction on the data sample $(\mathbf{x}_j, \mathbf{y}_j)$, where ℓ is the loss function.

As a typical scheme of differential privacy, the Gaussian mechanism can ensure that the output of the model has no significant statistical difference on the premise of effectively protecting the local dataset. Specifically, the original local model is protected by injecting Gaussian noise into the gradients of hidden layers during the training phase as follows

$$\nabla \hat{D}_s(\mathbf{W}^i) = \nabla D_s(\mathbf{W}^i) + N(0, \sigma_s^2), \quad (14)$$

where $\nabla \hat{D}_s(\mathbf{W}^i)$ is the encrypted average local gradient and σ_s^2 is the power of random noise for device s , which is independent and identically distributed (i.i.d.).

After the local training and encryption, all local models will be transmitted to the AP for model aggregation by

$$\mathbf{W}^{i+1} = \frac{1}{|\mathcal{O}_s|} \sum_{s=1}^S |\mathcal{O}_s| \mathbf{W}_s^i. \quad (15)$$

\mathbf{W}^{i+1} is the global model for $(i+1)$ -th training round, which will be downloaded to device $s = 1, 2, \dots, S$ as the initial configuration for round $i+1$, that is, $\mathbf{W}_1^{i+1} = \mathbf{W}_2^{i+1} = \dots = \mathbf{W}_S^{i+1} = \mathbf{W}^{i+1}$. The above process is repeated at each communication round until the converges, and finally the optimal DNN model \mathbf{W}_{opt} can be obtained.

Algorithm 1: The FDL Algorithm for the Parallel Optimization of Multiple IRSs

Training Phase:
for $IRS\ s = 1, 2, \dots, S$ **do**

Initialization of local models:

$$\mathbf{W}_1^1, \mathbf{W}_2^1, \dots, \mathbf{W}_S^1$$

end

// Repeat until convergence

for $IRS\ s = 1, 2, \dots, S$ **do**

 Train the local models $\mathbf{W}_1^i, \mathbf{W}_2^i, \dots, \mathbf{W}_S^i$ according to the local datasets $\mathcal{O}_1, \mathcal{O}_2, \dots, \mathcal{O}_S$ as (11)-(13);

Local models encryption as (14);

Upload local models and aggregating as (19);

 Broadcast the global model \mathbf{W}^{i+1} to all IRS as the initial configuration for next training round;

end
Inference Phase:
for $user\ k = 1, 2, \dots, K$ **do**

Send the current coordinates to AP;

end

AP: broadcast the coordinates bundle to all IRSs:

$$\Omega = \{(x_1, y_1), (x_2, y_2), \dots, (x_K, y_K)\}$$

for $IRS\ s = 1, 2, \dots, S$ **do**

 Load the optimal DNN model \mathbf{W}_{opt} ;

 Predict the optimal reflecting vector $\tilde{\Theta}_s$ with the input Ω ;

 Configure each elements according to $\tilde{\Theta}_s$;

end

In summary, the FDL algorithm for multiple IRSs to make the optimal IRS reflecting coefficients configuration is provided in Algorithm 1.

B. DNN and Training Dataset

In order to maximize the throughput of the system, each IRS needs to be adjusted to realize the optimal phase shift configuration $\{\Theta_1, \Theta_2, \dots, \Theta_S\}_{opt}$. Hence, it is necessary to establish a mapping relationship between the user and the reflection coefficient matrix of IRS.

In detail, the input of DNN is a bundle of coordinate information with respect to K users, i.e., $\Omega \triangleq \{(x_1, y_1), (x_2, y_2), \dots, (x_K, y_K)\}$. Actually, the coordinate information is related to the channel state information (CSI) as mentioned in Section III, which is highly correlated with the spatial location of the transceiver. In practical terms, these users' location coordinates are randomly selected from a set that contains all possible location points. As for the output of the DNN, i.e., the label of the training data, Θ_{opt} is the optimal reflection coefficient matrix of IRS. In order to facilitate the model design and reduce the computational redundancy, Θ is vectorized to $\tilde{\Theta}$, i.e., $\tilde{\Theta} = \text{diag}(\Theta)$. Therefore, the local

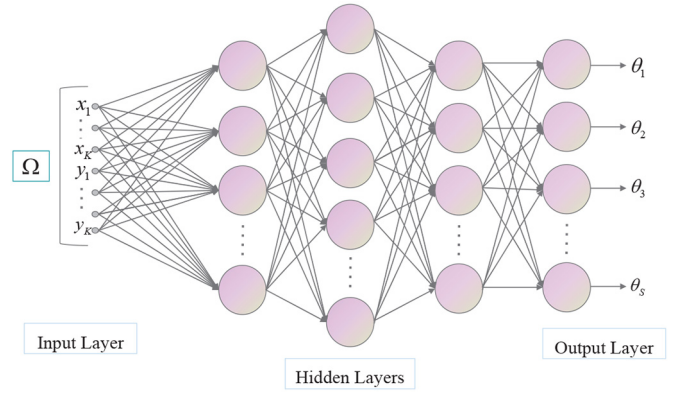


Fig. 4. The proposed DNN structure for configuration optimization of IRS.

dataset of s -th IRS can be represented as

$$\Psi_s = \left\{ \left(\Omega^1, \tilde{\Theta}^1 \right), \left(\Omega^2, \tilde{\Theta}^2 \right), \dots, \left(\Omega^{|\mathcal{O}_s|}, \tilde{\Theta}^{|\mathcal{O}_s|} \right) \right\}. \quad (16)$$

For Ψ_s , it contains $|\mathcal{O}_s|$ times random selection of coordinates.

The final issue is the acquisition of the training label $\tilde{\Theta}$. The exhaustive search of discrete fourier transform (DFT) codebook is adopted. The DFT matrix of IRS along y -axis (similarly for z -axis) is defined as

$$\text{DFT}_{N_y} = \begin{pmatrix} 1 & 1 & \dots & 1 \\ e^{j\pi \sin(\xi_0)} & e^{j\pi \sin(\xi_1)} & \dots & e^{j\pi \sin(\xi_{N_y-1})} \\ e^{j\pi 2 \sin(\xi_0)} & e^{j\pi 2 \sin(\xi_1)} & \dots & e^{j\pi 2 \sin(\xi_{N_y-1})} \\ \vdots & \vdots & \ddots & \vdots \\ e^{j\pi (N_y-1) \sin(\xi_0)} & e^{j\pi (N_y-1) \sin(\xi_1)} & \dots & e^{j\pi (N_y-1) \sin(\xi_{N_y-1})} \end{pmatrix}. \quad (17)$$

N_y is the number of IRS elements that distributed on the y -axis. Each ξ represents an AoA at y -axis of IRS and it varies between the interval $[-\frac{\pi}{2}, \frac{\pi}{2}]$, i.e., $\xi_0 = -\frac{\pi}{2}$ and $\xi_{N_y-1} = \frac{\pi}{2}$. Thus, the difference between the sine values of two adjacent incident angles is $\frac{2}{N_y}$ and the angle resolution of this DFT matrix can be obtained as

$$\xi_{res} = \arcsin\left(\frac{2}{N_y}\right). \quad (18)$$

It is worth noting that the antenna spacing in (17) is set as $\frac{\lambda}{2}$.

According to the above description, the DFT codebook Λ_{IRS} can be expressed as

$$\Lambda_{IRS} = \text{DFT}_{N_y} \otimes \text{DFT}_{N_z}. \quad (19)$$

The process of exhaustive search over Λ_{IRS} can be described as

$$\tilde{\Theta} = \text{vec} \left(\arg \max_{\Theta \in \Lambda_{IRS}} \sum_{k=1}^K \log_2(1 + \gamma_k) \right), \quad (20)$$

where $\text{vec}(\cdot)$ is the vectorization operation.

Since the input and the output are both vectors, the multi-layer-perceptron (MLP) is chosen as the basic DNN structure. Specifically, a five-layer MLP shown in Fig. 4 is adopted,

which consists of an input layer, three hidden layers, and an output layer. For the dimension of the input layer, it can be determined according to K . All hidden layers are fully connected layers, and the output layer is a regression layer. The neurons number of the i -th layer is denoted as $Z = \{Z_i\}_{i=1,2,3,4,5}$. Moreover, $\tanh(\cdot)$ is selected as the activation function. In the forward propagation stage, the coordinate combinations of K users and the corresponding optimal reflecting vector $\tilde{\Theta}$ are used as input and output respectively. Furthermore, the root mean squared error (RMSE) criterion is adopted to measure the error between the real output and the label, i.e.,

$$\ell = \left(\frac{1}{\varsigma} \sum_{j=1}^{\varsigma} \left\| \tilde{\Theta}_{out}^j - \tilde{\Theta}^j \right\|^2 \right)^{\frac{1}{2}}, \quad (21)$$

in which ς is the scale of test set and $\tilde{\Theta}_{out}$ denotes the real output of DNN. Meanwhile, the stochastic gradient descent (SGD) algorithm is employed for gradient descent.

In the inference phase, each IRS controller $s, s = 1, 2, \dots, S$ loads the optimal model \mathbf{W}_{opt} and the optimal reflecting combination $\{\tilde{\Theta}_1, \tilde{\Theta}_2, \dots, \tilde{\Theta}_S\}$ can be obtained. Then, all IRSs can adjust the phase shift of each element to realize the throughput maximization as (10).

C. Energy Consumption Model

Energy consumption is another major concern in this paper. Specifically, the energy consumption of two different schemes based on DL and FDL is analyzed, respectively. The total energy consumption is denoted as

$$E = E^t + E^c, \quad (22)$$

which mainly includes two parts: 1) the transmission energy consumption E^t and 2) the computation energy consumption E^c .

For simplicity and generality, we assume that the data rate of the control link between each IRS and AP is the same, which is recorded as r_t . Then, the transmission energy consumption under two different schemes can be written as

$$E_{DL}^t = \frac{P_{tr} Q_{DL}}{r_t}, \quad (23)$$

$$E_{FDL}^t = \frac{P_{tr} Q_{FDL}}{r_t}. \quad (24)$$

P_{tr} is the maximum transmit power of AP via the control link. Q represents the total transmitted symbols during the training process which can be further expressed as

$$Q_{DL} = \left(\sum_{s=1}^S |\mathcal{O}_s| \right) \left(|\Omega, \tilde{\Theta}| + |\mathbf{W}| S \right), \quad (25)$$

$$Q_{FDL} = 2|\mathbf{W}| T_{FDL} S. \quad (26)$$

For the Q_{DL} , the first term indicates the dataset transmission task from all IRSs to the AP, while the second term represents the download task after the model training. $|\Omega, \tilde{\Theta}|$ and $|\mathbf{W}|$ denote the parameter number of \mathbf{W} and one data point in \mathcal{O}_s , which will be accurately calculated in Section VI. T_{FDL}

represents the number of communication rounds required for the model convergence based on FDL.

On the other hand, the computation energy consumption based on DL and FDL can be given as

$$E_{DL}^c = T_{DL} P_{com}, \quad (27)$$

$$E_{FDL}^c = t_{lo} T_{FDL} S P_{com}, \quad (28)$$

where T_{DL} is the total time required for model convergence under the DL scheme. The training time for a single round that executed on a local device is denoted as t_{lo} . Besides, the total power of a device is P_{com} when performing training task. In (27) and (28), all IRS controllers are assumed to be homogeneous (i.e., the same computing performance). In addition, the energy consumed by model aggregation at the AP is ignored, because it only involves a small number of linear operations.

D. Computational Complexity

In this subsection, the computational complexity of the proposed algorithm is first calculated. Specifically, the time complexity of the FDL based algorithm at the inference phase can be represented as

$$\mathcal{O} \left(\sum_{i=1}^4 Z_i Z_{i+1} + Z_{i+1} \right), \quad (29)$$

It is worth noting that the time complexity of the DL based and FDL based algorithm at the inference phase is the same. However, the computation complexity of semi-definite relaxation (SDR) based algorithm and the lagrange dual decomposition (LDD) are in the order of $\mathcal{O}(N^6)$ [7], [33]. For alternating direction method of multipliers (ADMM) based algorithm [33], the time complexity is $\mathcal{O}(N^3)$. The N denotes the number of IRS elements.

By comparison, it is easy to see that the proposed FDL based algorithm has remarkable superiority in terms of computational complexity.

V. SIMULATION AND DISCUSSION

In this section, the simulation settings are first demonstrated, including the local dataset, the calculation of $|\Omega, \tilde{\Theta}|$, $|\mathbf{W}|$ and other parameters. Then, the rationality of FDL is revealed through the test accuracy and the comparison of convergence effects between DL and FDL. In addition, the simulation results verify the superiority of FDL over DL in terms of energy efficiency, and the effectiveness of FDL in the aspect of throughput maximization.

A. Simulation Settings

In this paper, the open dataset **DeepMIMO** [34] is used to generate the local dataset $\mathcal{O}_1, \mathcal{O}_2, \dots, \mathcal{O}_S$ and the 'O1' scenario is selected. **DeepMIMO** is an open real-world dataset and it precisely describes the authentic electromagnetic interaction characteristics in a given area. Besides, the **DeepMIMO** is based on the ray-tracing technology, which means it is 3D modeling and it is widely used in many prior works [35], [36]. Specifically, BS 7, 9, 10 are utilized as IRS

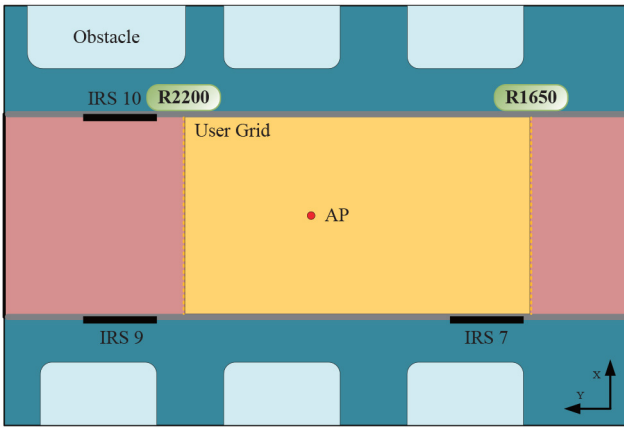


Fig. 5. The dataset construction based on the ray tracing scenario ‘O1’.

TABLE III
THE PARAMETERS OF THE LOCAL DATASET

Parameters	Value
System bandwidth	100MHz
Operating frequency	28GHz
OFDM limit	1
Sampling factor	1
Number of paths (L)	5
Antenna gain	3dBi

and the user grid is composed of the user point from R1650 to R2200 as illustrated in Fig. 5. For each data point (Ω, Θ) , the K coordinates of Ω are randomly selected in the user grid, which means it obeys i.i.d. for these data points. The transmitter at (R2000,90) is considered as an AP. Meanwhile, each data point in **DeepMIMO** includes two aspects: 1) coordinate information and 2) CSI (i.e., h_r^s, h_t^s and H^k). Hence, the optimal reflecting vector Θ can be obtained according to (19) and (20). The elements number of all IRSs is set to $N = 400$ (i.e., $N_y = N_z = 20$), and the number of users is $K = \{2, 4, 6, 8, 10, 12\}$. Suppose that the scale of each local dataset is the same, i.e., $|\mathcal{O}_1| = |\mathcal{O}_2| = \dots, |\mathcal{O}_S| = 5000$, 80% of which is the training set and 20% is the test set, the test set did not participate in the training process completely. Besides, the transmitting power of the AP over the control link is set to P_{tr} . The data rate of the control link is $r_t = 0.5$ Mbps. The rest of local dataset parameters are summarized in Table III.

As for $|\Omega, \Theta|$ and $|\mathcal{W}|$, they can be calculated as $2K + N$ and $\sum_{i=1}^4 (\kappa Z_i Z_{i+1} + 1)$, respectively. $\kappa = 0.5$ denotes the dropout probability between two layers and Z_i is the neurons number of i -th layer which is set as $Z = \{2K, 64, 256, 512, N\}$. $Z_i Z_{i+1}$ and Z_{i+1} represent the number of symbols for weight and bias.

B. Simulation Results

The test accuracy of the FDL algorithm for multiple IRSs is demonstrated in Fig. 6. In this simulation, we perform 1000

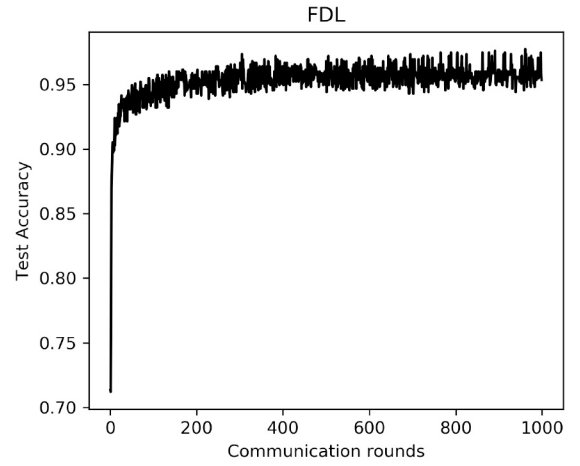


Fig. 6. The test accuracy versus communications rounds based on FDL framework.

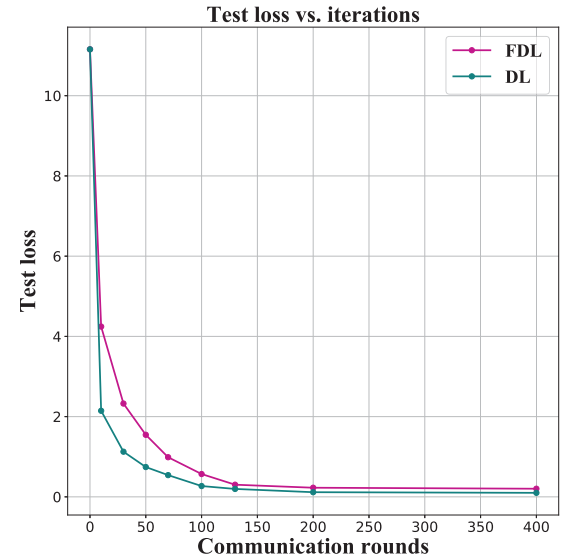


Fig. 7. The test loss versus communication rounds based on DL and FDL.

communication rounds. During a single communication round, each client executes 20 epochs to makeover the local dataset. The batch size of local updates is 200, and the learning rate is set to 0.01. The proposed FDL framework reaches 95.22% test accuracy after 200 communication rounds.

The test loss of the FDL framework is shown in Fig. 7. It is obvious that the proposed FDL algorithm can converge after 150 rounds of communication. The training loss of FDL stabilizes to 0.18 as demonstrated. Meanwhile, the rationality of the proposed FDL algorithm is verified based on the comparison of convergence performance with DL. It is clear that FDL can effectively approximate DL in terms of convergence speed and the final convergence value.

For the FL coupled with the real wireless network, we pay more attention to transmission energy consumption and spectrum occupancy. Therefore, the transmission overhead and the transmission energy consumption are recorded to verify the superiority of the proposed FDL over DL in terms of energy efficiency as illustrated in Fig. 8 and Fig. 9. In Fig. 8, multiple sets of experimental data under different numbers of IRS and users are plotted, respectively. Taking the experiment with

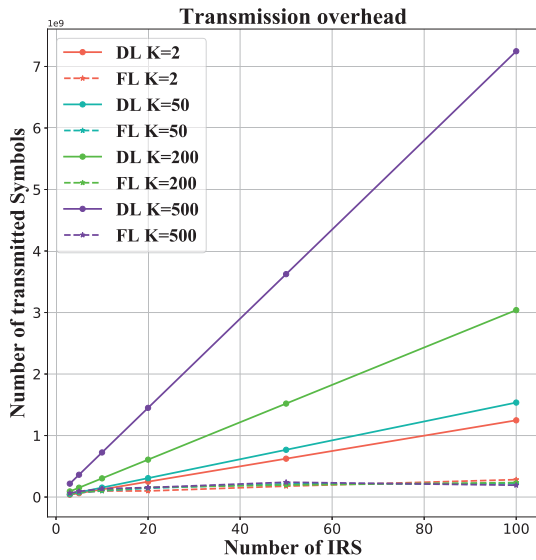


Fig. 8. The transmission overhead of DL and FDL.

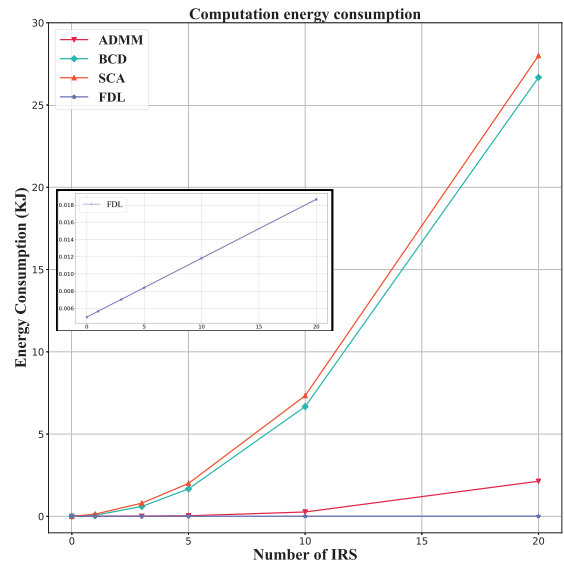


Fig. 10. The computation energy consumption versus the number of IRS (each IRS with $N = 40$ elements).

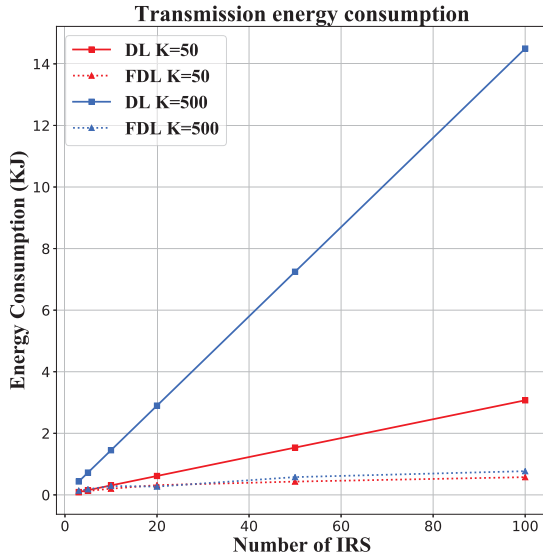


Fig. 9. The transmission energy consumption of DL and FDL.

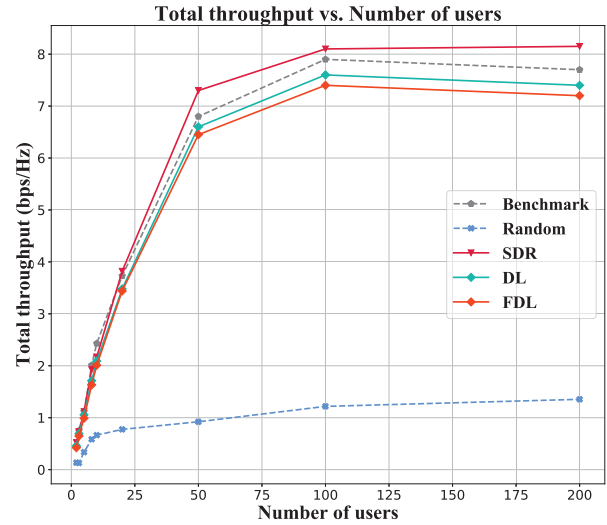


Fig. 11. The total throughput performance versus the number of users.

$K = 100, S = 10$ as an example, the number of transmitted symbols increases linearly with the number of IRS, and the slope depends on the number of users. The reason is that with the increase of the user number K , the transmitted symbols for each data point $[(\Omega, \Theta)]$ increases accordingly. Instead, there is no significant change for the FDL in terms of transmission overhead. Although the transmission burden will be heavier as the number of local devices increases, the number of communication rounds will also decrease accordingly, which will offset the negative effect. As shown in Fig. 9, the lowest transmission energy consumption of FDL is only 1/36 of that of DL when $K = 500$.

Besides, the superiority of the proposed FDL-based algorithm in computation energy consumption is also proved in Fig. 10. Specifically, the total energy consumption during a complete inference phase of the FDL approach is calculated. Meanwhile, this result is compared with some state-of-the-art

methods according to their computational complexity, including the ADMM, the block coordinate descent (BCD), and the SCA [33]. The power and frequency of the controller’s CPU are set to 100W and 3GHz. As shown in Fig. 10, the energy required for the FDL-based algorithm to complete an inference process is extremely low compared with other algorithms. The reason is that the number of required CPU cycles increases linearly with the number of IRS elements as we analyzed in (29). The computational complexity is reduced by orders of magnitude compared with other algorithms. Accordingly, to demonstrate more clearly the trend of the energy consumption of the FDL-based algorithm, a subplot is inserted in Fig. 10. As depicted in the subfigure, the FDL-based algorithm takes only 0.018 kJ to perform a complete optimization process for a scenario with 20 IRSs, which proves its great superiority in terms of energy efficiency.

Finally, Fig. 11 shows how the total network throughput changes with the number of users under different schemes.

Specifically, a benchmark using the label $\tilde{\Theta}$ for calculation is presented for comparison, which also represent the upper bound of the learning scheme. Besides, the strategy of randomly updating and the SDR based algorithm [7] are also performed for comparison. It can be observed that the total system throughput achieved based on the proposed FDL algorithm can reach 93% of the upper bound, and it can effectively approach the result based on the DL algorithm and SDR method. However, the total throughput will no longer increase or even decrease when K exceeds 100. There are two main reasons: 1) the angle resolution ξ_{res} of the DFT codebook Λ_{IRS} is not precise enough for such a large user group and 2) the intra-cell interference is too severe. In addition, the results obtained from the SDR algorithm will not present a downward trend owing to the infinite state space of the reflecting vector $\tilde{\Theta}$, which is different from the DFT codebook with discrete values.

VI. CONCLUSION

This paper proposes a novel FDL framework and algorithm to solve the optimal configuration problem for multiple IRSs assisted wireless communication networks. A DNN model is formulated to establish the mapping function between the coordinate information of users and the optimal reflecting vector of IRS. In the FDL framework, the model parameters are transmitted instead of the original dataset as in the DL scheme, which can effectively reduce the transmission overhead and the energy consumption. The simulation results have verified that the proposed algorithm can effectively reduce the energy consumption with attractive test accuracy. In addition, the total throughput of the communication system based on the proposed FDL algorithm can reach 93% of the theoretical performance.

REFERENCES

- [1] Q. Wu and R. Zhang, "Towards smart and reconfigurable environment: Intelligent reflecting surface aided wireless network," *IEEE Commun. Mag.*, vol. 58, no. 1, pp. 106–112, Jan. 2020.
- [2] S. Gong *et al.*, "Toward smart wireless communications via intelligent reflecting surfaces: A contemporary survey," *IEEE Commun. Surveys Tuts.*, vol. 22, no. 4, pp. 2283–2314, 4th Quart., 2020.
- [3] Q. Wu, S. Zhang, B. Zheng, C. You, and R. Zhang, "Intelligent reflecting surface-aided wireless communications: A tutorial," *IEEE Trans. Commun.*, vol. 69, no. 5, pp. 3313–3351, May 2021.
- [4] B. Di, H. Zhang, L. Li, L. Song, Y. Li, and Z. Han, "Practical hybrid beamforming with finite-resolution phase shifters for reconfigurable intelligent surface based multi-user communications," *IEEE Trans. Veh. Technol.*, vol. 69, no. 4, pp. 4565–4570, Apr. 2020.
- [5] B. Di, H. Zhang, L. Song, Y. Li, Z. Han, and H. V. Poor, "Hybrid beamforming for reconfigurable intelligent surface based multi-user communications: Achievable rates with limited discrete phase shifts," *IEEE J. Sel. Areas Commun.*, vol. 38, no. 8, pp. 1809–1822, Aug. 2020.
- [6] W. Yan, X. Yuan, Z.-Q. He, and X. Kuai, "Passive beamforming and information transfer design for reconfigurable intelligent surfaces aided multiuser MIMO systems," *IEEE J. Sel. Areas Commun.*, vol. 38, no. 8, pp. 1793–1808, Aug. 2020.
- [7] Q. Wu and R. Zhang, "Intelligent reflecting surface enhanced wireless network: Joint active and passive beamforming design," in *Proc. IEEE Global Commun. Conf. (GLOBECOM)*, Abu Dhabi, United Arab Emirates, Dec. 2018, pp. 1–6.
- [8] L. Li *et al.*, "Enhanced reconfigurable intelligent surface assisted mmWave communication: A federated learning approach," *China Commun.*, vol. 17, no. 10, pp. 115–128, Oct. 2020.
- [9] C. Pradhan, A. Li, L. Song, B. Vucetic, and Y. Li, "Hybrid Precoding design for reconfigurable intelligent surface aided mmWave communication systems," *IEEE Wireless Commun. Lett.*, vol. 9, no. 7, pp. 1041–1045, Jul. 2020.
- [10] G. Zhou, C. Pan, H. Ren, K. Wang, and A. Nallanathan, "A framework of robust transmission design for IRS-aided MISO communications with imperfect cascaded channels," *IEEE Trans. Signal Process.*, vol. 68, pp. 5092–5106, Aug. 2020.
- [11] H. Liu, X. Yuan and Y.-J. A. Zhang, "Matrix-calibration-based cascaded channel estimation for reconfigurable intelligent surface assisted multiuser MIMO," *IEEE J. Sel. Areas Commun.*, vol. 38, no. 11, pp. 2621–2636, Nov. 2020.
- [12] Y. Yang, S. Zhang, and R. Zhang, "IRS-enhanced OFDMA: Joint resource allocation and passive beamforming optimization," *IEEE Wireless Commun. Lett.*, vol. 9, no. 6, pp. 760–764, Jun. 2020.
- [13] Z. Yang *et al.*, "Resource Allocation for Wireless Communications with Distributed Reconfigurable Intelligent Surfaces," in *Proc. IEEE Global Commun. Conf. (GLOBECOM)*, Taipei, Taiwan, Dec. 2020, pp. 1–6.
- [14] M. Cui, G. Zhang, and R. Zhang, "Secure wireless communication via intelligent reflecting surface," *IEEE Wireless Commun. Lett.*, vol. 8, no. 5, pp. 1410–1414, Oct. 2019.
- [15] X. Yu, D. Xu, Y. Sun, D. W. K. Ng, and R. Schober, "Robust and secure wireless communications via intelligent reflecting surfaces," *IEEE J. Sel. Areas Commun.*, vol. 38, no. 11, pp. 2637–2652, Nov. 2020.
- [16] S. Misra, S. K. Roy, A. Roy, M. S. Obaidat, and A. Jha, "MEGAN: Multipurpose energy-efficient, adaptable, and low-cost wireless sensor node for the Internet of Things," *IEEE Syst. J.*, vol. 14, no. 1, pp. 144–151, Mar. 2020.
- [17] C. Huang, A. Zappone, G. C. Alexandropoulos, M. Debbah, and C. Yuen, "Reconfigurable intelligent surfaces for energy efficiency in wireless communication," *IEEE Trans. Wireless Commun.*, vol. 18, no. 8, pp. 4157–4170, Aug. 2019.
- [18] S. Hua, Y. Zhou, K. Yang, Y. Shi, and K. Wang, "Reconfigurable intelligent surface for green edge inference," *IEEE Trans. Green Commun. Netw.*, vol. 5, no. 2, pp. 964–979, Jun. 2021.
- [19] S. Jia, X. Yuan, and Y.-C. Liang, "Reconfigurable intelligent surfaces for energy efficiency in D2D communication network," *IEEE Wireless Commun. Lett.*, vol. 10, no. 3, pp. 683–687, Mar. 2021.
- [20] S. Sun, M. Fu, Y. Shi, and Y. Zhou, "Towards reconfigurable intelligent surfaces powered green wireless networks," in *Proc. IEEE Wireless Commun. Netw. Conf. (WCNC)*, Seoul, South Korea, Apr. 2020, pp. 1–6.
- [21] S. Zhou, W. Xu, K. Wang, M. D. Renzo, and M.-S. Alouini, "Spectral and energy efficiency of IRS-assisted MISO communication with hardware impairments," *IEEE Wireless Commun. Lett.*, vol. 9, no. 9, pp. 1366–1369, Sep. 2020.
- [22] J. Xiong, L. You, D. W. K. Ng, C. Yuen, W. Wang, and X. Gao, "Energy efficiency and spectral efficiency tradeoff in RIS-aided multiuser MIMO uplink systems," *Proc. IEEE Global Commun. Conf. (GLOBECOM)*, Taipei, Taiwan, Dec. 2020, pp. 1–6.
- [23] Z. Yang *et al.*, "Energy-efficient wireless communications with distributed reconfigurable intelligent surfaces," *IEEE Trans. Wireless Commun.*, early access, Jul. 27, 2021, doi: [10.1109/TWC.2021.3098632](https://doi.org/10.1109/TWC.2021.3098632).
- [24] L. You, J. Xiong, D. W. K. Ng, C. Yuen, W. Wang, and X. Gao, "Energy efficiency and spectral efficiency tradeoff in RIS-aided multiuser MIMO uplink transmission," *IEEE Trans. Signal Process.*, vol. 69, pp. 1407–1421, Dec. 2021.
- [25] G. Lee, M. Jung, A. T. Z. Kargari, W. Saad, and M. Bennis, "Deep reinforcement learning for energy-efficient networking with reconfigurable intelligent surfaces," in *Proc. IEEE Int. Conf. Commun. (ICC)*, Dublin, Ireland, Jun. 2020, pp. 1–6.
- [26] S. Khan and S. Y. Shin, "Deep-learning-aided detection for reconfigurable intelligent surfaces," 2020, [arXiv:1910.09136](https://arxiv.org/abs/1910.09136).
- [27] Q. Zhang, W. Saad, and M. Bennis, "Reflections in the sky: Millimeter wave communication with UAV-carried intelligent reflectors," in *Proc. IEEE Global Commun. Conf. (GLOBECOM)*, Waikoloa, HI, USA, Dec. 2019, pp. 1–6.
- [28] C. Huang, G. C. Alexandropoulos, C. Yuen, and M. Debbah, "Indoor signal focusing with deep learning designed reconfigurable intelligent surfaces," in *Proc. IEEE 20th Int. Workshop Signal Process. Adv. Wireless Commun. (SPAWC)*, Cannes, France, Jul. 2019, pp. 1–5.
- [29] D. Ma, L. Li, H. Ren, D. Wang, X. Li, and Z. Han, "Distributed rate optimization for intelligent reflecting surface with federated learning" in *Proc. IEEE Int. Conf. Commun. Workshops (ICC Workshops)*, Dublin, Ireland, Jun. 2020, pp. 1–6.
- [30] O. E. Ayach, S. Rajagopal, S. Abu-Surra, Z. Pi, and R. W. Heath, "Spatially sparse precoding in millimeter wave MIMO systems," *IEEE Trans. Wireless Commun.*, vol. 13, no. 3, pp. 1499–1513, Mar. 2014.

- [31] H. B. McMahan, E. Moore, D. Ramage, S. Hampson, and B. A. Y. Arcas, "Communication-efficient learning of deep networks from decentralized data," 2017, *arXiv:1602.05629*.
- [32] J. Zhao, Y. Chen, and W. Zhang, "Differential privacy preservation in deep learning: Challenges, opportunities and solutions," *IEEE Access*, vol. 7, pp. 48901–48911, 2019.
- [33] H. Guo, Y. Liang, J. Chen, and E. G. Larsson, "Weighted sum-rate maximization for intelligent reflecting surface enhanced wireless networks," in *Proc. IEEE Global Commun. Conf. (GLOBECOM)*, Waikoloa, HI, USA, Dec. 2019, pp. 1–6.
- [34] A. Alkhateeb, "DeepMIMO: A generic deep learning dataset for millimeter wave and massive MIMO applications," 2019, *arXiv:1902.06435*.
- [35] A. Taha, M. Alrabeiah, and A. Alkhateeb, "Enabling large intelligent surfaces with compressive sensing and deep learning," *IEEE Access*, vol. 9, pp. 44304–44321, 2021.
- [36] H. Hojatian, J. Nadal, J.-F. Frigon, and F. Leduc-Primeau, "Unsupervised deep learning for massive MIMO hybrid beamforming," *IEEE Trans. Wireless Commun.*, vol. 20, no. 11, pp. 7086–7099, Nov. 2021.



Lixin Li (Member, IEEE) received the B.S. degree (Hons.), the M.S. degree (Hons.), and the Ph.D. degree from Northwestern Polytechnical University (NPU), Xi'an, China, in 2001, 2004, and 2008, respectively. From 2009 to 2011, he was a Postdoctoral Research Fellow with NPU. In 2011, he joined the School of Electronics and Information, NPU, where he is currently a Full Professor and the Deputy Director of Department of Communication Engineering. In 2017, he held the visiting scholar position with the University of Houston, Houston,

TX, USA. He has authored or coauthored five books, more than 150 peer-reviewed papers in many prestigious journals and conferences, and he holds 20 granted patents. His current research interests include 5G/6G wireless networks, federated learning, game theory, and machine learning for wireless communications. He received the 2016 NPU Outstanding Young Teacher Award, which is the highest research and education honors for young faculties in NPU. He was an Exemplary Reviewer for IEEE TRANSACTIONS ON COMMUNICATIONS in 2020.



Donghui Ma is currently pursuing the master's degree with the School of Electronics and Information, Northwestern Polytechnical University, China, under supervision of Prof. L. Li. His research interests include intelligent reflecting surface enhanced communications and federated learning in wireless communication network.



Huan Ren received the B.Sc. degree in communication engineering and the M.Sc. degree in electronics and communication from Northwestern Polytechnical University, Xi'an, China, in 2018 and 2021, respectively, under the supervision of Prof. L. Li. She is currently an FPGA Engineer with the Beijing Institute of Telemetry Technology. Her research interests include satellite communications and on-board signal processing.



Peijue Wang is currently pursuing the master's degree with the School of Electronics and Information, Northwestern Polytechnical University, China, under supervision of Prof. L. Li. His research interests include reconfigurable intelligent surface and federated learning for communication and network.



Wensheng Lin (Member, IEEE) received the B.Eng. degree in communication engineering and the M.Eng. degree in electronic and communication engineering from Northwestern Polytechnical University, Xi'an, China, in 2013 and 2016, respectively, and the Ph.D. degree in information science from the Japan Advanced Institute of Science and Technology, Ishikawa, Japan, in 2019. He is currently an Associate Professor with the School of Electronics and Information, Northwestern Polytechnical University. His research interests

include network information theory, distributed source coding, and age of information.



Zhu Han (Fellow, IEEE) received the B.S. degree in electronic engineering from Tsinghua University in 1997, and the M.S. and Ph.D. degrees in electrical and computer engineering from the University of Maryland, College Park, in 1999 and 2003, respectively. From 2000 to 2002, he was an R&D Engineer of JDSU, Germantown, MD, USA. From 2003 to 2006, he was a Research Associate with the University of Maryland. From 2006 to 2008, he was an Assistant Professor with Boise State University, Boise, ID, USA. He is currently a John and Rebecca

Moores Professor with the Electrical and Computer Engineering Department and the Computer Science Department, University of Houston, Houston, TX, USA, and also with the Department of Computer Science and Engineering, Kyung Hee University, Seoul, South Korea. His research interests include wireless resource allocation and management, wireless communications and networking, game theory, big data analysis, security, and smart grid. He received an NSF Career Award in 2010, the Fred W. Ellersick Prize of the IEEE Communication Society in 2011, the EURASIP Best Paper Award for the *Journal on Advances in Signal Processing* in 2015, IEEE Leonard G. Abraham Prize in the field of Communications Systems (best paper award in IEEE JOURNAL ON SELECTED AREAS IN COMMUNICATIONS) in 2016, and several best paper awards in IEEE conferences. He is 1% highly cited researcher since 2017 according to Web of Science. He is also the winner of 2021 IEEE Kiyu Tomiyasu Award, for outstanding early to mid-career contributions to technologies holding the promise of innovative applications, with the following citation: "for contributions to game theory and distributed management of autonomous communication networks." He was an IEEE Communications Society Distinguished Lecturer from 2015 to 2018, and has been an AAAS Fellow since 2019 and a ACM Distinguished Member since 2019.